A placenta-on-a-chip model to determine the regulation of FKBPL and galectin-3 in preeclampsia

Masoumeh Ghorbanpour (masoumeh.s.ghorbanpour@student.uts.edu.au)
University of Technology Sydney https://orcid.org/0000-0001-5614-5215

Claire Richards
University of Technology Sydney

Dillan Pienaar
University of Technology Sydney

Kimberly Sesperez
University of Technology Sydney

Hamidreza Aboulkheyr Es.c
University of Technology Sydney

Valentina Nikolic
University of Niš: Univerzitet u Nisu

Natasa Karadzov Orlic
University of Belgrade: Univerzitet u Beogradu

Zeljko Mikovic
University of Belgrade: Univerzitet u Beogradu

Milan Stefanovic
University of Nis: Univerzitet u Nisu

Zoran Cakic
General hospital of Leskovac

Abdelrahim Alqudah
The Hashemite University

Louise Cole
University of Technology Sydney

Catherine Gorrie
University of Technology Sydney

Kristine McGrath
University of Technology Sydney

Mary M. Kavurma
The University of Sydney

Majid Ebrahimi Warkianib
University of Technology Sydney

Lana McClements

University of Technology Sydney https://orcid.org/0000-0002-4911-1014

Research Article

Keywords: microfluidics, placental development, preeclampsia, vascular remodeling, FKBPL, galectin-3

Posted Date: May 11th, 2022

DOI: https://doi.org/10.21203/rs.3.rs-1606096/v1

Version of Record: A version of this preprint was published at Cellular and Molecular Life Sciences on January 18th, 2023. See the published version at https://doi.org/10.1007/s00018-022-04648-w.

Abstract

Preeclampsia is a pregnancy-specific cardiovascular disorder and a leading cause of morbidity and mortality in pregnancy. Although inappropriate placental development and growth are recognized as root causes of preeclampsia, pathogenic mechanisms are poorly understood due to limited models of the disease, particularly in early pregnancy. Here, we first confirm the aberrant expression of important vascular and inflammatory proteins, FK506-binding protein like (FKBPL) and galectin-3 (Gal-3), in human plasma and placental tissue from women with/without preeclampsia. We then employ a 3D microfluidic placental model incorporating human umbilical vein endothelial cells (HUVECs) and a first trimester trophoblast cell line (ACH-3P) to investigate FKBPL and Gal-3 signalling in inflammatory conditions. In human samples, both circulating ($n = 17$ controls; $n = 30$ preeclampsia) and placental ($n \geq 6$) FKBPL and Gal-3 levels were increased in preeclampsia compared to heathy controls (plasma: FKBPL, $p < 0.0001$; Gal-3, $p < 0.01$; placenta: FKBPL, $p < 0.05$; Gal-3, $p < 0.01$), indicative of vascular dysfunction in preeclampsia. In our placenta-on-a-chip model, we show that endothelial cells are critical for trophoblast-mediated migration and that trophoblasts effectively remodel the vasculature recapitulating placental development. Inflammatory cytokine tumour necrosis factor-α (10ng/ml) modulates both FKBPL and Gal-3 signalling in conjunction with trophoblast migration and impairs vasculature ($p < 0.005$). Our placenta-on-a-chip recapitulates aspects of aberrant placentation in preeclampsia and represents a promising platform for further placental research.

Introduction

Preeclampsia is characterized by the new onset of high blood pressure in combination with proteinuria or organ dysfunction and can be categorized into an early-onset (diagnosed < 34-weeks gestation) or late-onset phenotype (diagnosed ≥ 34 weeks) [1]. In severe cases, preeclampsia can be life threatening during pregnancy and also leads to increased risk of both the mother and offspring developing cardiovascular and metabolic disorders later in life [2–5]. Currently, there are limited monitoring options for women at risk of preeclampsia and the only definitive treatment is the delivery of the placenta and baby, which is often preterm and carries its own complications. Though much of the etiology of preeclampsia is unknown, it is thought to have origins in inappropriate placentation and vascular dysfunction leading to systemic oxidative stress, inflammation, endothelial dysfunction and an anti-angiogenic environment [6].

During normal placental development, trophoblast cells invade the decidualized endometrial lining of the uterus to anchor the placenta and establish connection to the maternal circulation. An invasive subtype of trophoblasts, extravillous trophoblasts (EVTs), invade the spiral uterine arteries (SUAs) of the decidua and inner third of the myometrium in a tightly regulated fashion [7]. The vessels are subsequently remodeled, replacing the endothelial and muscle layers to reduce vessel resistance, resulting in unrestricted blood flow which facilitates the growth of the fetus during pregnancy [8]. However, impaired SUA remodeling has been observed in women with preeclampsia and is believed to play a key role in its pathogenesis, triggering a cascade of events following placental malperfusion [9]. For example, it has been shown that preeclampsia is associated with upregulation of inflammatory factors including tumor

necrosis factor alpha (TNF-α) and interleukin 6 (IL-6); cell adhesion molecules such as soluble vascular cell adhesion molecule 1 (sVCAM-1) and intercellular adhesion molecule 1 (sICAM-1); cellular fibronectin and anti-angiogenic proteins such as soluble fms-like tyrosine kinase-1 (sFlt-1), amongst others [6, 10–19]. Two emerging pathways including the pro-inflammatory galectin-3 (Gal-3) and the anti-angiogenic, FK506-binding protein like (FKBPL), have been implicated in preeclampsia and associated cardiovascular complications [20, 21].

FKBPL belongs to the immunophilin protein group and has been shown to have roles in the regulation of glucocorticoid, androgen and estrogen receptor signaling, stem cell differentiation, inflammation and inhibition of angiogenesis; the latter three mediated via the CD44 cell surface receptor [22–30]. Further, recent data has demonstrated that FKBPL could be used as a diagnostic and/or treatment target for cardiovascular diseases (CVDs), placental health and preeclampsia [20, 31–33]. We recently showed that plasma and placental FKBPL expression levels were significantly higher in a cohort of pregnant women with preeclampsia compared to normotensive pregnancies. We demonstrated that FKBPL expression analyzed against its target, CD44, as CD44/FKBPL ratio, could be used as a potential predictive and diagnostic tool for preeclampsia, although its role in the pathogenesis of preeclampsia requires further elucidation.

In addition, Gal-3 is a cytokine-like, immunoregulatory protein that is involved in various pathologies associated with inflammation including heart remodelling/disease and has been shown to have a potential as a biomarker of cardiovascular disease risk in women with preeclampsia [21, 34, 35]. The distribution of Gal-3 in normal and malignant trophoblasts[36–38], as well as its important roles in tissue remodeling [34, 35], tumor cell adhesion [39], cancer immune evasion [40], epithelial wound healing, cell migration [41–43], proliferation [44], and angiogenesis[45] have previously been demonstrated. While reports have identified an upregulation of Gal-3 in plasma and placental samples of women with preeclampsia versus normotensive pregnancies [46, 47], its mechanisms in the pathogenesis of this disease and future cardiovascular disease risk require further investigation [48].

Given the challenges with investigating the early placentation processes in humans due to increased miscarriage risk associated with chorionic villus sampling, mechanisms of placental development and growth are still poorly understood. Traditional two-dimensional (2D) *in vitro* assays and *in vivo* models have limitations due to their simplicity and inter-species differences, respectively [49–53]. Three-dimensional (3D) cell culture models more closely recapitulate the human tissue to study cell-cell and cell-matrix interactions and specifically, microfluidic devices and organ-on-a-chip platforms allow the dynamic *in vitro* representation of various physiological processes. 3D models can facilitate better understanding of cellular and molecular mechanisms of aberrant placentation and provide a platform for therapeutic screening for pregnancy-related disorders. Some microfluidic models have already been developed to represent placental cell interactions, as recently reviewed by Richardson *et al.* and Young *et al.*[54, 55], some of these perhaps lacking relevant cell types. The ACH-3P trophoblast cell line was developed by the fusion of primary first trimester trophoblasts with an established choriocarcinoma cell line and has been shown to have physiological characteristics reflective of their trophoblast origin with

the metabolic capacity of cancer cells. Here, for the first time, we sought to use this cell line to generate a placenta-on-a-chip 3D microfluidic platform to investigate (i) trophoblast-endothelial cell interactions during placental development, (ii) vascular formation during placental growth and (iii) FKBPL and Gal-3 mechanisms during these processes, particularly within inflammatory conditions, which are characteristic of preeclampsia (Fig. 1).

Materials And Methods

Human sample collection: Human plasma and placental samples were collected as part of a multicenter study including three hospitals in Serbia. Blood samples were collected from 47 participants from normotensive control pregnancies (n = 17) and pregnant women with preeclampsia (n = 30), prior to labor. Blood samples were collected in ethylenediaminetetraacetic acid (EDTA) tubes and centrifuged at 2,000 rpm for 15 minutes at 4°C to isolate plasma. The samples were stored at -80°C. The placentae were dissected following delivery, and two full thickness blocks (2x2cm) were collected and transferred to a -80°C freezer. Placental samples were chosen at random (n = 6 controls and n = 11 from women with preeclampsia) for determining protein expression of Gal-3 and FKBPL. Preeclampsia was defined according to the American College of Obstetricians and Gynecologists (ACOG) 2019 guidelines [56]. Clinical characteristics of maternal age, gestational age, maternal body mass index (BMI), systolic (sBP), diastolic (dBP) and mean arterial blood pressure (MABP) and gravidity are presented in supplementary information (Tables 1 and 2) according to sample group.

Table 1
Adjusted correlations for differences in gestational age and maternal age between normotensive and preeclamptic placentae

Placental samples	FKBPL		Gal-3	
	Pearson Correlation	Correlation controlled by GA and MA	Pearson Correlation	Correlation controlled by GA and MA
PE	r = 0.370	r = 0.519	r = 0.361	r = 0.356
	p = 0.144	**p = 0.047**	p = 0.155	p = 0.193

Bold indicates statistical significance (p < 0.05). Key: FKBPL, FK506-binding protein like; Gal-3, galectin-3; PE, preeclampsia; GA, gestational age; MA, maternal age.

Protein extraction from placental samples: For placental protein extraction, 100mg of placental tissue was homogenized in the presence of beads using 250µl of RIPA lysis buffer (50mM Tris-HCL, 150mM NaCl, 0.1% Triton, 0.5% Sodium deoxycholate, 0.1% SDS, pH = 8) containing 1% Halt Protease Inhibitor Cocktail (Thermo Fisher Scientific, USA) on ice for 30 minutes before samples were centrifuged at 14,000 rpm for 10 minutes at 4oC. The supernatant was collected and stored at -80°C for downstream analysis.

Cell culture: Human Umbilical Vein Endothelial Cells (HUVECs; Promocell, Germany) were maintained in microvascular endothelial cell growth media (EGMTM-2MV, Lonza, Switzerland). ACH-3P trophoblast cells were kindly donated by Professor Gernot Desoye (Graz Medical University, Austria) and were

maintained in Ham's F12 nutrient mix supplemented with 10% FBS and 1% penicillin-streptomycin (Thermo Fisher Scientific, UK). Both cell types were incubated in a 37°C humidified atmosphere with 5% CO2. Flasks approaching 90% confluence were passaged using 2X Trypsin (Thermo Fisher Scientific, USA) as cell dissociated reagent for HUVECs and StemPro Accutase (Thermo Fisher Scientific, UK) for ACH-3Ps. Every five passages, ACH-3P cells were treated with a selection medium containing azaserine (5.7 μM) and hypoxanthine (100 μM) to prevent the overgrowth of choriocarcinoma.

2D in vitro cell ACH-3P and HUVEC TNF-α treatment: ACH-3Ps or HUVECs at 90% confluence were starved overnight in Ham's F12 and EGMTM-2MV (Lonza, Switzerland, #CC-3202) containing 1% FBS, respectively. The following day, 200,000 ACH-3Ps or HUVECs were seeded per well in 12-well plates and were incubated at 37°C and 5% CO2 for 6 hours. Cells were treated with 10ng/ml TNF-α (Sigma-Aldrich, USA, cat. #T0157) for 24 or 72 hours with untreated cells used as a control. Intracellular protein was extracted using RIPA lysis buffer as described for protein extraction from placental samples. Every five passages, ACH-3Ps were treated with a selection medium containing azaserine (5.7uM; Sigma-Aldrich, USA) and hypoxanthine (100uM; Sigma-Aldrich, USA). No HUVECs and ACH-3Ps were used beyond passage 10 and 20, respectively.

3D-Microfluidic model of placenta: Microfluidic tissue culture devices were purchased from AIM Biotech (Singapore). This polydimethylsiloxane (PDMS) device consists of three microfluidic chambers each with two side parallel media channels (width 0.5 mm) and a central region called the gel channel (width 1.3 mm) with the height of 0.25 mm. An extracellular matrix (ECM) matrix solution containing 2.5 mg/ml collagen type I, 10X PBS, H_2O and NaOH (0.5N) at pH 7.4 was prepared and kept on ice to avoid polymerization. Afterwards, the ECM solution was mixed with $8x10^6$/mL HUVECs on ice and injected into the dedicated gel region of the device according to the manufacturer's protocols (https://aimbiotech.com/learn/general-protocols/) [57]. The device was incubated at 37°C and 5% CO2 for 40 minutes to allow gel polymerization via thermal cross-linking. The two side channels were filled with 120μl EGM^{TM}-2MV immediately after gel polymerization and the chips were incubated at 37°C and 5% CO2. The media was changed every 24 hours. To monitor the ACH-3Ps' invasion and effect on HUVECs microvascular formation, $2x10^6$/mL ACHP-3Ps were added to one of the media channels at time point zero and then the devices were incubated at 37°C and 5% CO2 overnight. Cells were also treated with 10ng/ml TNF-α for 24 or 72 hours, with untreated cells as a treatment control. As an experimental control, some devices were loaded with either ACH-3Ps or HUVECs alone.

Immunofluorescence staining: Cell culture medium was removed from the microfluidic devices prior to washing with PBS. Cells were fixed with 4% paraformaldehyde (PFA; Sigma-Aldrich, USA) for 15 minutes at 37°C followed by permeabilization with 0.1% Triton-X (Sigma-Aldrich, USA,) for 10 minutes at room temperature. To reduce non-specific binding, cells were blocked with blocking buffer containing 5% bovine serum albumin (Sigma-Aldrich, USA) and 3% normal goat serum (Invitrogen, USA) for 4 hours at room temperature. The cells were then probed with a combination of either galectin-3 (1:200; R&D Systems, USA, cat. #842759), FKBPL (1:200; Proteintech, USA, cat. #100601AP), CD31 (1:200; Abcam, UK, cat. #ab24590), EpCAM (1:200; Genesearch, AU, cat. #D1B3), and/or HLA-G (1:200; Bio-Rad, USA, cat.

#MCA2043) primary antibodies and incubated at 4°C overnight. Following washing, goat anti-rabbit IgG H&L (Alexa Fluor® 488, Abcam, cat. #150077) and goat anti-mouse IgG H&L (Alexa Fluor® 594, Abcam, cat. #150116) secondary antibodies were added for two hours at room temperature. Finally, the cell's nucleus was stained with DAPI (10µg/ml, Invitrogen, USA, cat. #D1306) for one hour at room temperature.

Widefield and Laser Scanning confocal microscopy: Fluorescence images were obtained using a Leica Stellaris confocal and Nikon TIE2 widefield fluorescence and transmitted light microscope. Confocal images were acquired with a 20X objectives with NA 1.45 with Nyquist sampling. Z stacks (0.2 µm optical slices) were acquired using a 0.5 AU pinhole. Widefield images were acquired with a 20X objectives with NA 0.75 and long working distance (2300 µm). Images were either deconvolved with NIS-Elements (version 5.3) using Richardson-Lucy method or clarified using NIS-Elements Clarify.ai [58]. The intensity of fluorescent signal, an indicator of protein expression, was analyzed using ImageJ software (NIH, USA, version 2.1.0). Network branching of endothelial microvasculature was analyzed using the Angiogenesis Analyzer macro on ImageJ [59].

Western blotting: Human placental and cell lysate protein samples were quantified using a bicinchoninic acid (BCA) assay (Thermo Scientific Pierce ^{TM} BCA Protein Assay Kit, #23225). Samples (20µg) were reduced with 4X Laemmli sample buffer (Bio-Rad, USA) and subjected to Western Blotting. Membranes were probed with mouse anti-FKBPL (1:1000; Proteintech, USA, cat. #663891Ig), or mouse anti-human galectin-3 (1:500; R&D Systems, USA, cat. 842759), or rabbit anti-Glyceraldehyde 3-phosphate dehydrogenase (GAPDH; 1:6000; Abcam, UK, cat. #ab37168) primary antibody in 5% skim milk overnight at 4^{o}C. Membranes were incubated with their corresponding secondary antibody, anti-mouse IgG (1:1,000; GE Healthcare, UK, cat. # NXA931) or anti-rabbit (Abcam, UK, cat. #ab6721) antibody and imaged by chemiluminescence using a ChemiDoc MP imaging system (Bio-Rad, USA). Band intensity was measured using ImageJ and normalized to the housekeeping protein, GAPDH.

FKBPL ELISA: Plasma from women with preeclampsia was analyzed for FKBPL concentration by sandwich ELISA and compared to that of normotensive controls. An FKBPL ELISA kit from Cloud-Clone Corp (#SEL523Hu, China) was used according to the manufacturer's instructions. Optical density was measured using a Spark 10M plate reader (Tecan, Switzerland) microplate reader at 450nm. The four-parameter logistic (4PL) curve regression model was used to determine concentration values of each sample from the sigmoidal standard curve.

Galectin-3 ELISA: The Gal-3 protein concentration of placental and in vitro supernatant samples was quantified using a galectin-3 DuoSet enzyme-linked immunosorbent assay (ELISA) kit (R&D Systems, USA, cat. #DY1154) according to the manufacturer's instructions. The absorbance was measured at 450nm and 540nm (reference wavelength) using a Spark 10M plate reader (Tecan, Switzerland). The four-parameter logistic (4PL) curve regression model was used to determine concentration values of each sample from the sigmoidal standard curve.

Statistical analysis: The results of human sample quantifications were presented as mean ± SD whereas the results of quantitative *in vitro* experiments were presented as mean ± SEM. Normality testing was performed using- a Shapiro-Wilks test followed by two-tailed unpaired t-test or one-way ANOVA or two-way ANOVA with post-hoc multiple comparison tests. For non-normally distributed data, Mann-Whitney or Kruskal-Wallis were used. Statistical analysis was performed using GraphPad Prism (version 8.4.3 software, USA) and p-value < 0.05 was considered statistically significant. An unpaired t-test was used to determine differences between gestational age, maternal age and BMI. Where there were statistically significant differences between the groups ($p < 0.05$), SPSS software (IBM 1.0.0.146, USA) was used to perform correlations between preeclampsia and FKBPL or Gal-3 plasma concentration or placental expression using Pearson's correlation and partial correlation controlling for these factors.

Results

Circulating and placental FKBPL and Gal-3 are increased in preeclampsia. To determine if FKBPL and Gal-3 expression was altered in preeclampsia compared to normotensive pregnancies, placental and plasma samples were interrogated by Western blotting and ELISA, respectively. With respect to variations between case (preeclampsia) and control groups, no differences in BMI were observed, however, gestational age was significantly lower and maternal age significantly higher in the preeclampsia group (Supplementary Table 1). Placental FKBPL protein expression was over two-fold higher from women with preeclampsia compared to normotensive controls (control 1.00 ± 0.22 vs preeclampsia 2.28 ± 1.99, fold change, $p = 0.02$; Fig. 2A and Supplementary Fig. 1). Although no correlation was observed between placental FKBPL protein expression and preeclampsia ($r = 0.370$, $p = 0.144$), this became statistically significant after adjusting for confounders including gestational and maternal age ($r = 0.519$, $p = 0.047$, Table 1). Similarly, placental Gal-3 protein expression was increased in the preeclampsia group (control 167.4 ± 56.7 vs preeclampsia 498.2 ± 531.5, pg/ml, $p = 0.004$; Fig. 1B), however, no correlation between placental Gal-3 expression and preeclampsia was observed ($r = 0.361$, $p = 0.155$), even when adjusted for gestational and maternal age ($r = 0.356$, $p = 0.193$; Table 1).

Whilst there were no differences in maternal age between the normotensive and preeclampsia plasma samples, gestational age was significantly lower and body mass index (BMI) significantly higher in the preeclampsia group (supplementary Table 2). Plasma samples analysed by ELISA demonstrated a significant increase in FKBPL concentration in women with preeclampsia compared to normotensive pregnancies (control 0.88 ± 0.35 vs preeclampsia 1.41 ± 0.42, ng/ml, $p < 0.0001$; Fig. 1C and supplementary Fig. 1). Further, there was a significant positive correlation between plasma FKBPL and preeclampsia ($r = 0.578$, $p < 0.001$), even when adjusted for differences in gestational age and BMI ($r = 0.559$, $p < 0.001$; Table 2). Similarly, plasma Gal-3 concentration from women with preeclampsia compared to controls was also increased (control 222.2 ± 72.91 vs preeclampsia 288.8 ± 71.98, pg/ml, $p = 0.004$; Fig. 1E). Aligned to this, plasma Gal-3 concentration was positively correlated with preeclampsia ($r = 0.389$, $p = 0.007$), although the statistical significance was lost when adjusted for differences in gestational age and BMI as confounding factors ($r = 0.281$, $p = 0.064$; Table 2).

Inflammation regulates FKBPL and Gal-3 expression in trophoblast and endothelial cell 2D monocultures. To investigate the regulation of FKBPL and Gal-3 under inflammatory conditions, trophoblasts (ACH-3Ps) or human umbilical vein endothelial cells (HUVECs) were treated with TNF-α (10ng/ml), an inflammatory stimulus elevated in preeclampsia,[14] for 24 to 72 hours. FKBPL protein expression was significantly increased ~ 1.5-fold, in ACH-3Ps at both time points (control 1.00 ± 0.074 vs TNF-α-24h 1.65 ± 0.16 vs TNF-α-72h 1.58 ± 0.13, fold change, p = 0.021; Fig. 3A, B and supplementary Fig. 2). TNF-α exposure also stimulated Gal-3 protein expression by ~ 2.5-fold in ACH-3Ps exposed to 24 hour TNF-α however this increase was non-significant by 72 hours (control 0.751 ± 0.23 vs TNF-α-24h 2.40 ± 0.33 vs TNF-α-72h 2.00 ± 0.454, fold change, p = 0.036; Fig. 3A, C and supplementary Fig. 2).

Similarly, FKBPL protein expression was increased in HUVECs ~ 2-fold following 24 hours of TNF-α treatment and was maintained at 72 hours (control 0.84 ± 0.12 vs TNF-α-24h 1.84 ± 0.28 vs TNF-α-72h 1.76 ± 0.12, fold change, p = 0.03; Fig. 3D, E and supplementary Fig. 3). When we examined Gal-3 protein expression in HUVECs, there was a trend towards an increase in Gal-3 following 24 hour exposure to TNF-α, though this did not become significant until it increased by ~ 2-fold at 72 hours (control 0.65 ± 0.01 vs TNF-α-24h 1.10 ± 0.14 vs TNF-α-72h 1.54 ± 0.12, fold change, p = 0.006; Fig. 3D, F and supplementary Fig. 3).

Trophoblast migration is stimulated by the presence of endothelial cells or inflammatory conditions. We next used our placenta-on-a-chip model to assess the invasion and migratory ability, as well as regulation of FKBPL and Gal-3, under inflammatory conditions (typical of preeclampsia), of trophoblasts in the absence and presence of endothelial cells. ACH-3Ps were added to one of the media channels whereas the extracellular matrix (ECM) solution with and without HUVECs was placed in the middle channel (Fig. 4A). Cells were treated with 10ng/ml TNF-α for 24 or 72 hours, with untreated cells as a treatment control (Fig. 4B). ACH-3Ps were limited in their invasion through the collagen matrix without HUVECs present and in the absence of TNF-α (Fig. 4A-1 and B). TNF-α exposure stimulated a significant increase in ACH-3Ps migration at both time points (control 130.3 ± 11.23 vs TNF-α-24h 252 ± 41.67 vs TNF-α-72h 269.3 ± 43.6, p = 0.0039; Fig. 4A-1 and C).

When HUVECs were added to the central matrix channel, ACH-3Ps actively traversed the collagen matrix across the chip, and there were no differences in ACH-3Ps migration exposed to inflammatory conditions (Fig. 4A-2, B and C). Interestingly, there was a significant increase in the number of migrating trophoblasts in the presence of endothelial cells, as determined by cytokeratin 7 staining (without HUVECs vs with HUVECs; Control 130.3 ± 11.23 vs 799 ± 8.71, TNF-α-24h 252 ± 41.67 vs 761 ± 18.66, TNF-α-72h 269.3 ± 43.6 vs 838 ± 7.93, p < 0.0001; Fig. 4C).

In the 3D monoculture microfluidics ACH-3P system, FKBPL protein expression was significantly reduced with TNF-α treatment at 24 hours before it was restored and increased by 72 hours (control 1.00 ± 0.04 vs TNF-α-24h 0.35 ± 0.05 vs TNF-α-72h 1.25 ± 0.03, fold change, p < 0.0001; Fig. 4A-1, D and supplementary Fig. 4A). However, in the co-culture system, the presence of endothelial cells increased the FKBPL expression of trophoblasts following 24 hours of TNF-α treatment which was reduced by 72 hours

(control 0.91 ± 0.1 vs TNF-α-24h 1.63 ± 0.09 vs TNF-α-72h 0.63 ± 0.02, fold change, p < 0.0001; Fig. 4A-2, E and supplementary Fig. 5A). A similar effect was observed for Gal-3 expression in the absence (control 1.00 ± 0.05 vs TNF-α-24h 0.41 ± 0.05 vs TNF-α-72h 1.34 ± 0.06, fold change, p < 0.0001; Fig. 4A-1,F and supplementary Fig. 4B) and presence of endothelial cells (control 1.00 ± 0.06 vs TNF-α-24h 2.10 ± 0.15 vs TNF-α-72h 0.98 ± 0.09, fold change, p p < 0.0001, Fig. 4A-2, G and supplementary Fig. 5B). However, there was no difference in Gal-3 expression between the control and 72 h TNF-α treatment (Fig. 4G).

Endothelial cells spontaneously form microvascular networks within microfluidics chips that are impacted by the presence of ACH-3P cells and inflammatory conditions. In order to investigate mechanisms of placental growth and vasculature, our next step was to examine microvascular network formation of HUVECs both in the presence and absence of ACH-3Ps, and/or inflammation (Fig. 5A1 and A2). Immunofluorescent microscopy showed intricate microvascular network formation by endothelial cells with junctions between branches (Fig. 5A and B). Within the microfluidic environment without ACH-3Ps (Fig. 5A-1), 24-hour TNF-α treatment had no effect on endothelial FKBPL protein expression, however, after 72 hours FKBPL protein expression was reduced by ~ 4-fold (control 1.00 ± 0.1 vs TNF-α-24h 1.12 ± 0.05 vs TNF-α-72h 0.28 ± 0.01, fold change, p < 0.0001; Fig. 5A-1, B and C). However, in the co-culture system (Fig. 5A-2), the presence of trophoblast cells and TNF-α treatment increased the FKBPL expression of HUVECs following 24 hours of TNF-α treatment which was reduced significantly by 72 hours (control 1.00 ± 0.08 vs TNF-α-24h 1.50 ± 0.11 vs TNF-α-72h 0.18 ± 0.01, fold change, p < 0.0001; Fig. 5A-2, D and supplementary Fig. 7A). In the 3D monoculture microfluidics HUVEC system, there was no difference in endothelial Gal-3 protein expression within 24-hour TNF-α treatment, however, after 72 hours, Gal-3 protein expression was also reduced by ~ 4-fold (control 1.00 ± 0.01 vs TNF-α-24h 0.77 ± 0.13 vs TNF-α-72h 0.17 ± 0.02, fold change, p = 0.0006; Fig. 5A-1, E and supplementary Fig. 6). Similar to FKBPL expression, when ACH-3Ps were introduced to microfluidic chips, TNF-α treatment for 24 hours led to an initial increase in Gal-3 expression of HUVECs by ~ 2.5-fold that was significantly reduced by 72 hours (control 1.00 ± 0.16 vs TNF-α-24h 2.34 ± 0.09 vs TNF-α-72h 0.41 ± 0.02, fold change, p < 0.0001; Fig. 5A-2, F and supplementary Fig. 7B).

When there were no trophoblast cells in the system, there was a significant increase in CD31 protein expression of HUVECs following 24 hours of TNF-α treatment, which was reduced significantly by 72 hours (control 1.00 ± 0.07 vs TNF-α-24h 1.25 ± 0.04 vs TNF-α-72h 0.29 ± 0.02, fold change, p < 0.0001; Fig. 5A-1, B and G). In the presence of ACH-3Ps a progressive decrease in CD31 expression following TNF-α treatment was observed (control 1.00 ± 0.07 vs TNF-α-24h 0.57 ± 0.11 vs TNF-α-72h 0.05 ± 0.004, fold change, p = 0.0004; Fig. 5A-2, H and supplementary Fig. 7A) in the system. FKBPL is known to have an anti-angiogenic function,[18] therefore an increase in FKBPL at 24 hours likely led to inhibited vasculature and hence CD31 expression at 72 hours, which initiated a downregulation of FKBPL as a result of compensatory mechanism to restore angiogenesis.

We also examined the 3D HUVECs monoculture and co-culture microvascular network structures within microfluidics chips by measuring the number of master segments, master junctions and total isolated branches using an Angiogenesis Analyzer macro.[54] There was a significant difference in 3D HUVECs

monoculture and co-culture microvascular network structures and following 72 h TNF- α treatment including the number of master segments (-ACH3Ps vs + ACH-3Ps; control 636.3 ± 47.32 vs 409.8 ± 10.7, TNF-α-24h 616.7 ± 6.7 vs 320.6 ± 10.4, TNF-α-72h 327.7 ± 63.7 vs 82.3 ± 11.68, $p < 0.0001$; Fig. 6A and B), number of master junctions (-ACH-3Ps vs + ACH-3Ps; control 297.3 ± 16.5 vs 204.3 ± 19.4, TNF-α-24h 274.7 ± 3.3 vs 184.2 ± 5.3, TNF-α-72h 163.7 ± 24.6 vs 99.7 ± 16.60, $p < 0.0001$; Fig. 6C) and total isolated branches (-ACH-3Ps vs + ACH-3Ps; control 1575 ± 232.4 vs 397.0 ± 65.2, TNF-α-24h 2352 ± 219.3 vs 495.8 ± 102.4, TNF-α-72h 3223 ± 114.6 vs 4568 ± 539.9, $p < 0.0001$; Fig. 6D). The vast majority of these results show reduction in microvascular growth in our placenta-on-a-chip model in the presence of trophoblast cells or TNF- α (Fig. 6B and C), which is reflective of SUA remodeling during placental development. However, prolonged TNF-α treatment (72h) in addition to inducing reduced placental microvascular growth, also impaired the vasculature measured by the increase in isolated branches, which is even more pronounced in the presence of ACH-3Ps (Fig. 6D).

Discussion

Despite extensive research, there has been a lack of definitive prophylactic and curative treatment options for preeclampsia during pregnancy. This has, in part, been due to difficulties in obtaining human samples of the early placenta and the lack of biologically relevant model systems of human disease. Consequently, establishing a reliable and representative model of the early placenta to study mechanisms leading to preeclampsia remains important towards developing better monitoring and treatment strategies for women and babies affected by preeclampsia. In this study we utilized a placenta-on-a-chip model that recapitulates placental development (through ACH-3P trophoblast migration and invasion), growth (endothelial cell/HUVEC-initiated vasculature development) and an inflammatory human placenta. Importantly, in our study we showed that (i) there is an upregulation of novel vascular- and inflammation-related proteins, FKBPL and Gal-3, in both placenta and plasma samples collected from women with preeclampsia compared to normotensive controls, (ii) endothelial and trophoblast interactions can affect changes in FKBPL and Gal-3 protein expression patterns and (iii) inflammation and upregulation of FKBPL and Gal-3 is associated with impaired microvasculature network formation and placental growth. All of these aberrant placental changes can lead to preeclampsia.

As mentioned above, FKBPL has been shown to have roles in the regulation of steroid receptor signaling, cell differentiation and inhibition of angiogenesis [23–29]. In our previous study, we observed that plasma FKBPL was reduced early in pregnancy (15 weeks gestation) in women who proceeded to develop preeclampsia; while following diagnosis (> 20 weeks) FKBPL was significantly increased in plasma and placentae compared to healthy controls [20]. Here, we confirmed that following diagnosis of preeclampsia, FKBPL expression was significantly increased in the plasma and placentae of our new validation group of women with preeclampsia compared to normotensive controls. Additionally, we have recently shown the increased expression of FKBPL in the hearts of pregnant rats with reduced uterine perfusion pressure (RUPP), an *in vivo* model of preeclampsia, and cardiac spheroids treated with plasma from women with preeclampsia [32]. Given that FKBPL has anti-angiogenic properties, increased levels of FKBPL are associated with restricted angiogenesis, which is a hallmark of preeclampsia.

Furthermore, in our study we observed significantly increased levels of Gal-3 in placenta samples from women with preeclampsia compared to controls. Gal-3 is a known immunomodulatory protein and its specific structure facilitates the binding of ECM glycans to cell surfaces during tissue remodeling [34, 60]. Thus, we hypothesize that this altered phenotype could be reflective of placental adverse tissue remodeling leading to fibrosis, induced by increased inflammation, which are characteristic features of preeclampsia [61], although this would require further tissue analysis. In addition, we found circulating levels of Gal-3 in the plasma of women with preeclampsia to be significantly increased, in line with published literature [46–48]. Gal-3 has been shown to not only regulate tissue remodeling particularly in cardiovascular disease, but an increase in plasma Gal-3 correlates with conventional cardiovascular risk factors [62, 63]. Therefore, the increased levels of Gal-3 in the plasma from women with preeclampsia could represent an important mechanism leading to maternal cardiovascular remodeling and increased risk of future cardiovascular disease. While in our study there was no statistically significant correlation between Gal-3 secretion and preeclampsia, this could have been influenced by gestational age and suggests that Gal-3 expression changes throughout the time course of pregnancy, which has been previously observed [64, 65].

In our 2D monoculture experiments, we observed that inflammatory cytokine TNF-α upregulated both FKBPL and Gal-3 in trophoblasts and endothelial cells individually, similar to what is happening in human placenta in the presence of preeclampsia. To our knowledge, this regulatory effect of TNF-α on the expression of FKBPL has not previously been shown. Along with emerging evidence identifying FKBPL's role in regulating nuclear factor-κB (NF-κB) signaling, this could contribute to our understanding of the importance of FKBPL in inflammatory pathways [30]. On the other hand, the regulation of TNF-α by Gal-3 has been shown before [66–68], and various studies suggest that Gal-3 is under the positive control of TNF-α, for example, in plasma from patients with acute myocardial infarction there was an increased level of both TNF-α and Gal-3 [69–71]. Within the context of pregnancy, in *in vitro* trophoblast experiments, TNF-α was shown to upregulate Gal-3 expression while Gal-3 overexpression was also shown to upregulate TNF-α [72]. Thus, these data suggest Gal-3 and TNF-α regulate each other by a positive feedback mechanism and may contribute to inflammatory processes in preeclampsia.

Three-dimensional microfluidic models of the placenta incorporating the use of ECM components that provide structural support, cell-cell and cell-matrix interactions closer to that of *in situ* tissues have been developed [73]. For example, Lee *et al.* generated a placenta-on-a-chip model in a vertical co-culture configuration by adding human choriocarcinoma cell line, JEG-3, and HUVEC cells in media channels separated by an ECM channel [74]. From this, they were able to analyze the transport of glucose across the microengineered placenta barrier. However, JEG-3 are a cancer-derived cell line and are limited in their ability to physiologically reflect trophoblast cells. Further, the positioning of the two adherent cultures separated by ECM prevented the formation of microvasculature by the endothelial cells, as we have been able to demonstrate, and the vertical stacking of these channels poses imaging difficulties. On the other hand, another group developed a microfluidic model to study the migratory characteristics of EVTs by embedding primary, human first trimester trophoblasts in a central ECM channel [75]. While this model enabled the researchers to investigate important regulatory processes involved in early placental

development, with particular application to disorders of placentation such as preeclampsia, obtaining samples and the isolation and maintenance of these primary cell cultures is difficult and requires many supporting factors.

Considering this, we incorporated first trimester trophoblast cells, ACH-3Ps, HUVECs and inflammatory factors to generate a placenta-on-a-chip model and study novel mechanisms of placental development and growth, particularly relevant for preeclampsia development. Inflammatory conditions were also applied to recapitulate a critical aspect of the preeclamptic placenta. Like in the adherent monoculture setting, TNF-α treatment induced an increase in FKBPL in both trophoblasts and endothelial cells. Interestingly, while 24 hour exposure to TNF-α induced a significant increase in FKBPL in the trophoblasts grown in 2D, the microfluidic delivery of this inflammatory stimulus appeared to result in a delayed effect when HUVECs were not present. This delay was not seen, however when HUVECs were present in the chip, indicating a potential regulatory role of the endothelial cells on FKBPL trophoblast expression. Meanwhile, the initial increase in FKBPL protein expression by HUVECs correlated with the diminished angiogenic potential of these cells, as demonstrated by reduced master segments and master junctions; their ability to form new vessels from existing vessel structures. This effect is consistent with previous findings that *Fkbpl* knockout mice are embryonic lethal, whilst *Fkbpl* heterozygous mouse embryos exhibit impaired/leaky vasculature, strongly suggesting that FKBPL plays an essential role in developmental and physiological angiogenesis [26]. Whether the subsequent reduction in FKBPL expression at 72 h indicates a compensatory decrease to enable the stimulation of angiogenesis requires further investigation. These data suggest that endothelial-trophoblast interactions in our model have a key role in regulating placental development, angiogenesis and growth.

Gal-3 expression within the microfluidic device exhibited a similar expression pattern to FKBPL in the microfluidics chips carrying ACH-3Ps with or without HUVECs. Ultimately, Gal-3 expression was significantly decreased by 72-hours. This effect might be due the dynamic environment of the microfluidics device that prevents Gal-3 from building up given that the medium was changed every 24 hours. Our findings demonstrate that our 3D cell culture models using microfluidic devices are beneficial in studying complex pathophysiology under different treatments and conditions in real-time, as they provide a highly controllable dynamic microenvironment that prevents biomolecule accumulation in the ECM [76]. This is particularly important as endothelial cells are well established for sensing their mechanical environment as well as responding to biochemical signals [77].

In our placenta-on-a-chip model, we demonstrated that TNF-α treatment in HUVECs monocultures increased the expression of endothelial marker CD31, whereas CD31 expression was decreased in endothelial and trophoblast co-culture conditions. Pan-endothelial CD31 is an important vascular cell adhesion and signaling molecule that regulates endothelial cell migration, survival and maintenance of the endothelial cell permeability barrier [78]. Whether the reduction we noted is due to endothelial cell death induced by TNF-α [79, 80] or trophoblast cells [81, 82], or simply reduced expression in functional endothelial cells remains to be answered. However, placentae and decidua from women with preeclampsia, particularly with decidual vasculopathy, have shown to express reduced levels of CD31, an

indication of failed angiogenesis [83]. In line with this, the addition of TNF-α to our microfluidic system increased FKBPL and Gal-3 expression and impaired the ability of HUVECs to form continuous microvascular networks, as seen in the increase in the length of isolated branches, which are unable to establish appropriate junctions with nearby vessels. According to our data, an initial upregulation of antiangiogenic related protein, FKBPL, can interfere with the inflammation-induced angiogenesis process which leads to vascular complications in the preeclamptic placenta.

Our findings demonstrate that this 3D microfluidic model is an adaptable system for investigating complex pathophysiology under different treatments and conditions, as it provides a highly controllable, dynamic microenvironment and permits the observation of cellular interactions and behavior in real-time. One limitation of the model we present is the potential influence of the choriocarcinoma component of the ACH-3P cell line and the absence of primary cells. However, the incorporation of the immortalized ACH-3P line enabled us to generate a low-risk, low-cost and reproducible model of first trimester trophoblast and endothelial cell interactions in early placentation. Moreover, physiological or pathological primary cultures, additional cell types including stromal, glandular epithelial and immune cells or the addition of other key factors in preeclampsia such as sFlt-1 could improve the complexity of the model.

Conclusions

We developed an innovative and dynamic placenta-on-a-chip model incorporating immortalized first trimester trophoblast and endothelial cells, which are key cells for placental development and growth. We developed this model to resemble the preeclamptic placenta by including an important inflammatory factor, TNF-α, secreted by immune cells and shown to be increased in preeclampsia. This system can be made more complex by the incorporation of other cell types involved in placentation including fibroblasts, pericytes, decidual natural killer cells and macrophages to broaden our understanding of the pathogenesis of preeclampsia. We also validated this model by evaluating the emerging FKBPL and Gal-3 inflammatory and anti-angiogenic mechanisms in placental development and growth, compared to their secretion and expression in plasma and placental samples from women with preeclampsia. The application of microfluidic systems in evaluating angiogenesis and trophoblast invasion, a hallmark features of successful pregnancy, was also demonstrated. Our placenta-on-a-chip model can be utilized in the future for biomarker discovery and improving our understanding of the mechanisms involved in placental growth and development. Importantly, this platform will allow high-throughput screening of various therapeutic agents for conditions such as preeclampsia that currently have no definitive treatments. Moreover, this platform can reduce the use of animals in research investigating placental development and enable safe, low-cost and reliable testing of novel therapeutic agents for pregnancy conditions affected by aberrant placentation.

Declarations

Acknowledgements

The authors gratefully acknowledge the use of the Nikon TIE2 widefield and Leica Stellaris confocal microscope in the Microbial Imaging Facility (MIF) at the iThree institute in the Faculty of Science, the University of Technology Sydney. We would like to thank Dr Amy Bottomley for their scientific input and/or technical assistance. The authors would like to acknowledge the use of BioRender for the creation of the graphical abstract and schematics used in figures.

Author contributions

SG designed, optimised, and carried out the experiments, analysed and interpreted the data and wrote the manuscript. CR designed and carried out the experiments, analysed and interpreted the data and wrote the manuscript. DP and KS performed experiments and acquired and analysed the data. HA contributed to experiment design and optimisation, and provided significant intellectual contribution. VN, NO, ZM, MS, ZC coordinated and acquired clinical data and provided significant input on clinical data analysis and interpretation. AA acquired, processed and analysed the data. LC and CG contributed significantly to data acquisition and analysis. MW and LM conceptualised the study, designed the study and interpreted the data. LM, KM and MK supervised SG and CR and contributed to the data interpretation and manuscript writing. All authors approved the final version of the manuscript.

S.G. and C.R. contributed equally to this work.

Funding

This research was supported by Australian Government Research Training Program Scholarships, UTS Research Excellence (CR), International Research Scholarship (SG), UTS President Scholarship (SG) and the Faculty of Science Seed Funding (UTS).

Data availability

All the data generated or analysed during this study are available from the corresponding author upon resealable request.

Ethical approval and consent to participate

Ethical approval for this project was obtained from the University of Technology Sydney (UTS) Human Research Ethics Executive Review Committee and local hospital ethics committees. The study was conducted with the informed consent of each participant.

Conflicts of interest

The authors declare no financial conflict of interest. LM is an inventor on FKBPL-related patents.

Consent for publication

All the authors have consented for the publication in the CMLS.

References

1. Say L, Chou D, Gemmill A et al (2014) Global causes of maternal death: a WHO systematic analysis. Lancet Glob Heal 2:e323–e333. https://doi.org/10.1016/S2214-109X(14)70227-X
2. Metzger BE, Contreras M, Sacks DA et al (2008) Hyperglycemia and Adverse Pregnancy Outcomes. N Engl J Med 358:1991–2002. https://doi.org/10.1056/NEJMoa0707943
3. Catalano PM, McIntyre HD, Cruickshank JK et al (2012) The hyperglycemia and adverse pregnancy outcome study: Associations of GDM and obesity with pregnancy outcomes. Diabetes Care 35:780–786. https://doi.org/10.2337/dc11-1790
4. Yogev C, Hadden, Persson R (2010) Hyperglycemia and Adverse Pregnancy Outcome (HAPO) study: preeclampsia. Am J Obstet Gynecol 202:255.e1-255.e7. https://doi.org/10.1016/j.ajog.2010.01.024
5. Alqudah A, McKinley MC, McNally R et al (2018) Risk of pre-eclampsia in women taking metformin: a systematic review and meta-analysis. Diabet Med 35:160–172
6. Pennington KA, Schlitt JM, Jackson DL et al (2012) Preeclampsia: multiple approaches for a multifactorial disease. Dis Model Mech 5:9–18. https://doi.org/10.1242/dmm.008516
7. Pollheimer J, Vondra S, Baltayeva J et al (2018) Regulation of Placental Extravillous Trophoblasts by the Maternal Uterine Environment. Front Immunol 9:2597. https://doi.org/10.3389/fimmu.2018.02597
8. Osol G, Mandala M (2009) Maternal uterine vascular remodeling during pregnancy. Physiology 24:58–71
9. Burton GJ, Woods AW, Jauniaux E, Kingdom JCP (2009) Rheological and physiological consequences of conversion of the maternal spiral arteries for uteroplacental blood flow during human pregnancy. Placenta 30:473–482. https://doi.org/10.1016/j.placenta.2009.02.009
10. Halim A, Kanayama N, El Maradny E et al (1996) Plasma P selectin (GMP-140) and glycocalicin are elevated in preeclampsia and eclampsia: Their significances. Am J Obstet Gynecol 174:272–277. https://doi.org/10.1016/S0002-9378(96)70407-6
11. Saito S, Umekage H, Sakamoto Y et al (1999) Increased T-helper-1-type immunity and decreased T-helper-2-type immunity in patients with preeclampsia. Am J Reprod Immunol 41:297–306. https://doi.org/10.1111/j.1600-0897.1999.tb00442.x
12. Friedman SA, Schiff E, Emeis JJ et al (1995) Biochemical corroboration of endothelial involvement in severe preeclampsia. Am J Obstet Gynecol 172:202–203. https://doi.org/10.1016/0002-9378(95)90113-2
13. Islami D, Shoukir Y, Dupont P et al (2001) Is cellular fibronectin a biological marker for pre-eclampsia? Eur J Obstet Gynecol Reprod Biol 97:40–45. https://doi.org/10.1016/S0301-2115(00)00501-7
14. Chaiworapongsa T, Romero R, Yoshimatsu J et al (2002) Soluble adhesion molecule profile in normal pregnancy and pre-eclampsia. J Matern neonatal Med Off J Eur Assoc Perinat Med Fed Asia Ocean Perinat Soc Int Soc Perinat Obstet 12:19–27. https://doi.org/10.1080/jmf.12.1.19.27

15. Austgulen R, Lien E, Vince G, Redman CWG (1997) Increased maternal plasma levels of soluble adhesion molecules (ICAM-1, VCAM-1, E-selectin) in preeclampsia. Eur J Obstet Gynecol Reprod Biol 71:53–58. https://doi.org/https://doi.org/10.1016/S0301-2115(96)02647-4
16. Habas K, Shang L (2018) Alterations in intercellular adhesion molecule 1 (ICAM-1) and vascular cell adhesion molecule 1 (VCAM-1) in human endothelial cells. Tissue Cell 54:139–143. https://doi.org/10.1016/j.tice.2018.09.002
17. Blann AD (2006) Plasma von Willebrand factor, thrombosis, and the endothelium: the first 30 years. Thromb Haemost 95:49–55
18. Hlubocká Z, Umnerová V, Heller S et al (2002) Circulating intercellular cell adhesion molecule-1, endothelin-1 and von Willebrand factor-markers of endothelial dysfunction in uncomplicated essential hypertension: the effect of treatment with ACE inhibitors. J Hum Hypertens 16:557–562. https://doi.org/10.1038/sj.jhh.1001403
19. Kupferminc MJ, Peaceman AM, Wigton TR et al (1994) Tumor necrosis factor-α is elevated in plasma and amniotic fluid of patients with severe preeclampsia. Am J Obstet Gynecol 170:1752–1759. https://doi.org/10.1016/S0002-9378(12)91845-1
20. Todd N, McNally R, Alqudah A et al (2021) Role of A Novel Angiogenesis FKBPL-CD44 Pathway in Preeclampsia Risk Stratification and Mesenchymal Stem Cell Treatment. J Clin Endocrinol Metab 106:26–41. https://doi.org/10.1210/clinem/dgaa403
21. Atakul N, Atamer Y, Selek Ş et al (2021) ST2 and galectin-3 as novel biomarkers for the prediction of future cardiovascular disease risk in preeclampsia. J Obstet Gynaecol (Lahore) 0:1–7. https://doi.org/10.1080/01443615.2021.1991293
22. Annett S, Moore G, Short A et al (2020) FKBPL-based peptide, ALM201, targets angiogenesis and cancer stem cells in ovarian cancer. Br J Cancer 122:361–371. https://doi.org/10.1038/s41416-019-0649-5
23. Yakkundi A, McCallum L, O'Kane A et al (2013) The anti-migratory effects of FKBPL and its peptide derivative, AD-01: regulation of CD44 and the cytoskeletal pathway. PLoS ONE 8:e55075. https://doi.org/10.1371/journal.pone.0055075
24. McClements L, Yakkundi A, Papaspyropoulos A et al (2013) Targeting Treatment-Resistant Breast Cancer Stem Cells with FKBPL and Its Peptide Derivative, AD-01, via the CD44 Pathway. Clin Cancer Res 19:3881–3893. https://doi.org/10.1158/1078-0432.CCR-13-0595
25. McClements L, Annett S, Yakkundi A et al (2019) FKBPL and its peptide derivatives inhibit endocrine therapy resistant cancer stem cells and breast cancer metastasis by downregulating DLL4 and Notch4. BMC Cancer 19:351. https://doi.org/10.1186/s12885-019-5500-0
26. Yakkundi A, Bennett R, Hernández-Negrete I et al (2015) FKBPL is a critical antiangiogenic regulator of developmental and pathological angiogenesis. Arterioscler Thromb Vasc Biol 35:845–854. https://doi.org/10.1161/ATVBAHA.114.304539
27. McKeen HD, McAlpine K, Valentine A et al (2008) A Novel FK506-Like Binding Protein Interacts with the Glucocorticoid Receptor and Regulates Steroid Receptor Signaling. Endocrinology 149:5724–

5734. https://doi.org/10.1210/en.2008-0168

28. Sunnotel O, Hiripi L, Lagan K et al (2010) Alterations in the steroid hormone receptor co-chaperone FKBPL are associated with male infertility: a case-control study. Reprod Biol Endocrinol 8:22. https://doi.org/10.1186/1477-7827-8-22
29. Valentine A, O'Rourke M, Yakkundi A et al (2011) FKBPL and Peptide Derivatives: Novel Biological Agents That Inhibit Angiogenesis by a CD44-Dependent Mechanism. Clin Cancer Res 17:1044–1056. https://doi.org/10.1158/1078-0432.CCR-10-2241
30. Annett S, Spence S, Garciarena C et al (2021) The immunophilin protein FKBPL and its peptide derivatives are novel regulators of vascular integrity and inflammation via NF-κB signaling. https://doi.org/10.1101/2021.02.24.431422. bioRxiv
31. Andrzej S, Januszewski CJ, Watson, Vikki O'Neill K, McDonald M, Ledwidge T, Robson, Alicia J, Jenkins ACKM, and LM (2020) FKBPL is associated with metabolic parametersis a novel determinant of cardiovascular disease. Sci Rep Accepted
32. Richards C, Sesperez K, Chhor M et al (2021) Characterisation of Cardiac Health in the Reduced Uterine Perfusion Pressure Model and a 3. D Cardiac Spheroid Model, of Preeclampsia
33. Alqudah A, Eastwood K-A, Jerotic D et al (2021) FKBPL and SIRT-1 Are Downregulated by Diabetes in Pregnancy Impacting on Angiogenesis and Endothelial Function. Front Endocrinol (Lausanne) 12. https://doi.org/10.3389/fendo.2021.650328
34. Li LC, Li J, Gao J (2014) Functions of galectin-3 and its role in fibrotic diseases. J Pharmacol Exp Ther 351:336–343
35. Andrejic OM, Vucic RM, Pavlovic M et al (2019) Association between Galectin-3 levels within central and peripheral venous blood, and adverse left ventricular remodelling after first acute myocardial infarction. Sci Rep 9:13145. https://doi.org/10.1038/s41598-019-49511-4
36. Bozić M, Petronijević M, Milenković S et al (2004) Galectin-1 and galectin-3 in the trophoblast of the gestational trophoblastic disease. Placenta 25:797–802. https://doi.org/10.1016/j.placenta.2004.03.006
37. Vićovac L, Janković M, Cuperlović M (1998) Galectin-1 and – 3 in cells of the first trimester placental bed. Hum Reprod 13:730–735. https://doi.org/10.1093/humrep/13.3.730
38. Jeschke U, Mayr D, Schiessl B et al (2007) Expression of galectin-1, -3 (gal-1, gal-3) and the Thomsen-Friedenreich (TF) antigen in normal, IUGR, preeclamptic and HELLP placentas. Placenta 28:1165–1173. https://doi.org/10.1016/j.placenta.2007.06.006
39. Henderson NC, Mackinnon AC, Farnworth SL et al (2008) Galectin-3 expression and secretion links macrophages to the promotion of renal fibrosis. Am J Pathol 172:288–298. https://doi.org/10.2353/ajpath.2008.070726
40. CD29 and CD7 mediate galectin-3-induced type II T-cell apoptosis - PubMed
41. Danella Polli C, Alves Toledo K, Franco LH et al (2013) Monocyte Migration Driven by Galectin-3 Occurs through Distinct Mechanisms Involving Selective Interactions with the Extracellular Matrix. ISRN Inflamm 2013:1–9. https://doi.org/10.1155/2013/259256

42. Yabuta C, Yano F, Fujii A et al (2014) Galectin-3 enhances epithelial cell adhesion and wound healing in rat cornea. Ophthalmic Res 51:96–103. https://doi.org/10.1159/000355846
43. Gao X, Balan B, Tai G, Raz A (2014) Galectin-3 induces cell migration via a calcium-sensitive MAPK/ERK1/2 pathway. Oncotarget 5:2077–2084. https://doi.org/10.18632/oncotarget.1786
44. Inohara H, Akahani S, Raz A (1998) Galectin-3 stimulates cell proliferation. Exp Cell Res 245:294–302. https://doi.org/10.1006/excr.1998.4253
45. Jia W, Kidoya H, Yamakawa D et al (2013) Galectin-3 accelerates M2 macrophage infiltration and angiogenesis in tumors. Am J Pathol 182:1821–1831. https://doi.org/10.1016/j.ajpath.2013.01.017
46. Pankiewicz K, Szczerba E, Fijalkowska A et al (2020) The association between serum galectin-3 level and its placental production in patients with preeclampsia. J Physiol Pharmacol an Off J Polish Physiol Soc 71. https://doi.org/10.26402/jpp.2020.6.08
47. Taha AS, Zahraei Z, Al-Hakeim HK (2020) Serum apelin and galectin-3 in preeclampsia in Iraq. Hypertens Pregnancy 39:379–386. https://doi.org/10.1080/10641955.2020.1777300
48. Suvakov S, Bonner E, Nikolic V et al (2020) Overlapping Pathogenic Signalling Pathways and Biomarkers in Preeclampsia and Cardiovascular Disease. https://doi.org/10.1016/j.preghy.2020.03.011. Pregnancy Hypertens
49. Weimar CHE, Post Uiterweer ED, Teklenburg G et al (2013) In-vitro model systems for the study of human embryo-endometrium interactions. Reprod Biomed Online 27:461–476. https://doi.org/10.1016/j.rbmo.2013.08.002
50. Orendi K, Kivity V, Sammar M et al (2011) Placental and trophoblastic in vitro models to study preventive and therapeutic agents for preeclampsia. Placenta 32:S49–S54. https://doi.org/https://doi.org/10.1016/j.placenta.2010.11.023
51. Abbas Y, Turco MY, Burton GJ, Moffett A (2020) Investigation of human trophoblast invasion in vitro. Hum Reprod Update 26:501–513. https://doi.org/10.1093/humupd/dmaa017
52. Barry JS, Rozance PJ, Anthony RV (2008) An animal model of placental insufficiency-induced intrauterine growth restriction. Semin Perinatol 32:225–230. https://doi.org/10.1053/j.semperi.2007.11.004
53. Belkacemi L, Jelks A, Chen C-H et al (2011) Altered placental development in undernourished rats: role of maternal glucocorticoids. Reprod Biol Endocrinol 9:105. https://doi.org/10.1186/1477-7827-9-105
54. Richardson L, Kim S, Menon R, Han A (2020) Organ-On-Chip Technology: The Future of Feto-Maternal Interface Research? https://doi.org/10.3389/fphys.2020.00715. Front Physiol 11:
55. Young RE, Huh DD (2021) Organ-on-a-chip technology for the study of the female reproductive system. Adv Drug Deliv Rev 173:461–478. https://doi.org/https://doi.org/10.1016/j.addr.2021.03.010
56. ACOG Practice Bulletin No. 202: Gestational Hypertension and Preeclampsia.Obstet Gynecol133:e1–e25. https://doi.org/10.1097/AOG.0000000000003018

57. AIM Biotech Gel Filling. https://aimbiotech.com/2-gel-filling/
58. Nikon I (2020) Nikon introduces Clarify.ai for NIS-Elements, an artificial intelligence algorithm for removing blur from widefield microscope images. https://www.microscope.healthcare.nikon.com/about/news/nikon-introduces-clarify-ai-for-nis-elements-an-artificial-intelligence-algorithm-for-removing-blur-from-widefield-microscope-images
59. Carpentier G (2012) Angiogenesis Analyzer for ImageJ. http://image.bio.methods.free.fr/ImageJ/?Angiogenesis-Analyzer-for-ImageJ
60. Henderson NC, Sethi T (2009) The regulation of inflammation by galectin-3. Immunol Rev 230:160–171
61. Ohmaru-Nakanishi T, Asanoma K, Fujikawa M et al (2018) Fibrosis in Preeclamptic Placentas Is Associated with Stromal Fibroblasts Activated by the Transforming Growth Factor-B1 Signaling Pathway. Am J Pathol 188:683–695. https://doi.org/10.1016/j.ajpath.2017.11.008
62. de Boer RA, van Veldhuisen DJ, Gansevoort RT et al (2012) The fibrosis marker galectin-3 and outcome in the general population. J Intern Med 272:55–64. https://doi.org/10.1111/j.1365-2796.2011.02476.x
63. Sanchez-Mas J, Lax A, Asensio-Lopez MC et al (2014) Galectin-3 expression in cardiac remodeling after myocardial infarction. Int J Cardiol 172:e98–e101. https://doi.org/10.1016/j.ijcard.2013.12.129
64. Demmert M, Faust K, Bohlmann MK et al (2012) Galectin-3 in cord blood of term and preterm infants. Clin Exp Immunol 167:246–251. https://doi.org/10.1111/j.1365-2249.2011.04509.x
65. Freitag N, Tirado-Gonzalez I, Barrientos G et al (2020) Galectin-3 deficiency in pregnancy increases the risk of fetal growth restriction (FGR) via placental insufficiency. Cell Death Dis 11:560. https://doi.org/10.1038/s41419-020-02791-5
66. Hao M, Li M, Li W (2017) Galectin-3 inhibition ameliorates hypoxia-induced pulmonary artery hypertension. Mol Med Rep 15:160–168. https://doi.org/10.3892/mmr.2016.6020
67. Forsman H, Islander U, Andréasson E et al (2011) Galectin 3 aggravates joint inflammation and destruction in antigen-induced arthritis. Arthritis Rheum 63:445–454. https://doi.org/10.1002/art.30118
68. Volarevic V, Milovanovic M, Ljujic B et al (2012) Galectin-3 deficiency prevents concanavalin A-induced hepatitis in mice. Hepatology 55:1954–1964. https://doi.org/10.1002/hep.25542
69. Deschildre C, Ji JW, Chater S et al (2007) Expression of galectin-3 and its regulation in the testes. Int J Androl 30:28–40. https://doi.org/10.1111/j.1365-2605.2006.00707.x
70. Alturfan AA, Basar I, Emekli-Alturfan E et al (2014) Galectin-3 and plasma cytokines in patients with acute myocardial infarction. Lab Med 45:336–341. https://doi.org/10.1309/LM3JZKBDA7D4QFOC
71. Nishi Y, Sano H, Kawashima T et al (2007) Role of galectin-3 in human pulmonary fibrosis. Allergol Int 56:57–65. https://doi.org/10.2332/allergolint.O-06-449
72. Miyauchi M, Ao M, Furusho H et al (2018) Galectin-3 Plays an Important Role in Preterm Birth Caused by Dental Infection of Porphyromonas gingivalis. Sci Rep 8:2867. https://doi.org/10.1038/s41598-

018-21072-y

73. Mittal R, Woo FW, Castro CS et al (2019) Organ-on-chip models: Implications in drug discovery and clinical applications. J Cell Physiol 234:8352–8380. https://doi.org/10.1002/jcp.27729
74. Lee JS, Romero R, Han YM et al (2016) Placenta-on-a-chip: a novel platform to study the biology of the human placenta. J Matern neonatal Med Off J Eur Assoc Perinat Med Fed Asia Ocean Perinat Soc Int Soc Perinat Obstet 29:1046–1054. https://doi.org/10.3109/14767058.2015.1038518
75. Abbas Y, Oefner CM, Polacheck WJ et al (2017) A microfluidics assay to study invasion of human placental trophoblast cells. J R Soc Interface 14. https://doi.org/10.1098/rsif.2017.0131
76. Calibasi Kocal G, Güven S, Foygel K et al (2016) Dynamic Microenvironment Induces Phenotypic Plasticity of Esophageal Cancer Cells Under Flow. Sci Rep 6:38221. https://doi.org/10.1038/srep38221
77. Discher DE, Janmey P, Wang Y-L (2005) Tissue cells feel and respond to the stiffness of their substrate. Science 310:1139–1143. https://doi.org/10.1126/science.1116995
78. Lertkiatmongkol P, Liao D, Mei H et al (2016) Endothelial functions of platelet/endothelial cell adhesion molecule-1 (CD31). Curr Opin Hematol 23:253–259. https://doi.org/10.1097/MOH.0000000000000239
79. Robaye B, Mosselmans R, Fiers W et al (1991) Tumor necrosis factor induces apoptosis (programmed cell death) in normal endothelial cells in vitro. Am J Pathol 138:447–453
80. Winn RK, Harlan JM (2005) The role of endothelial cell apoptosis in inflammatory and immune diseases. J Thromb Haemost 3:1815–1824. https://doi.org/10.1111/j.1538-7836.2005.01378.x
81. Kuo C-Y, Shevchuk M, Opfermann J et al (2019) Trophoblast-endothelium signaling involves angiogenesis and apoptosis in a dynamic bioprinted placenta model. Biotechnol Bioeng 116:181–192. https://doi.org/10.1002/bit.26850
82. Ashton SV, Whitley GSJ, Dash PR et al (2005) Uterine Spiral Artery Remodeling Involves Endothelial Apoptosis Induced by Extravillous Trophoblasts Through Fas/FasL Interactions. Arterioscler Thromb Vasc Biol 25:102–108. https://doi.org/10.1161/01.ATV.0000148547.70187.89
83. Liu H, Li Y, Zhang J et al (2015) The defect of both angiogenesis and lymphangiogenesis is involved in preeclampsia. Placenta 36:279–286. https://doi.org/10.1016/j.placenta.2014.12.013

Table 2

Table 2 is not available with this version.

Figures

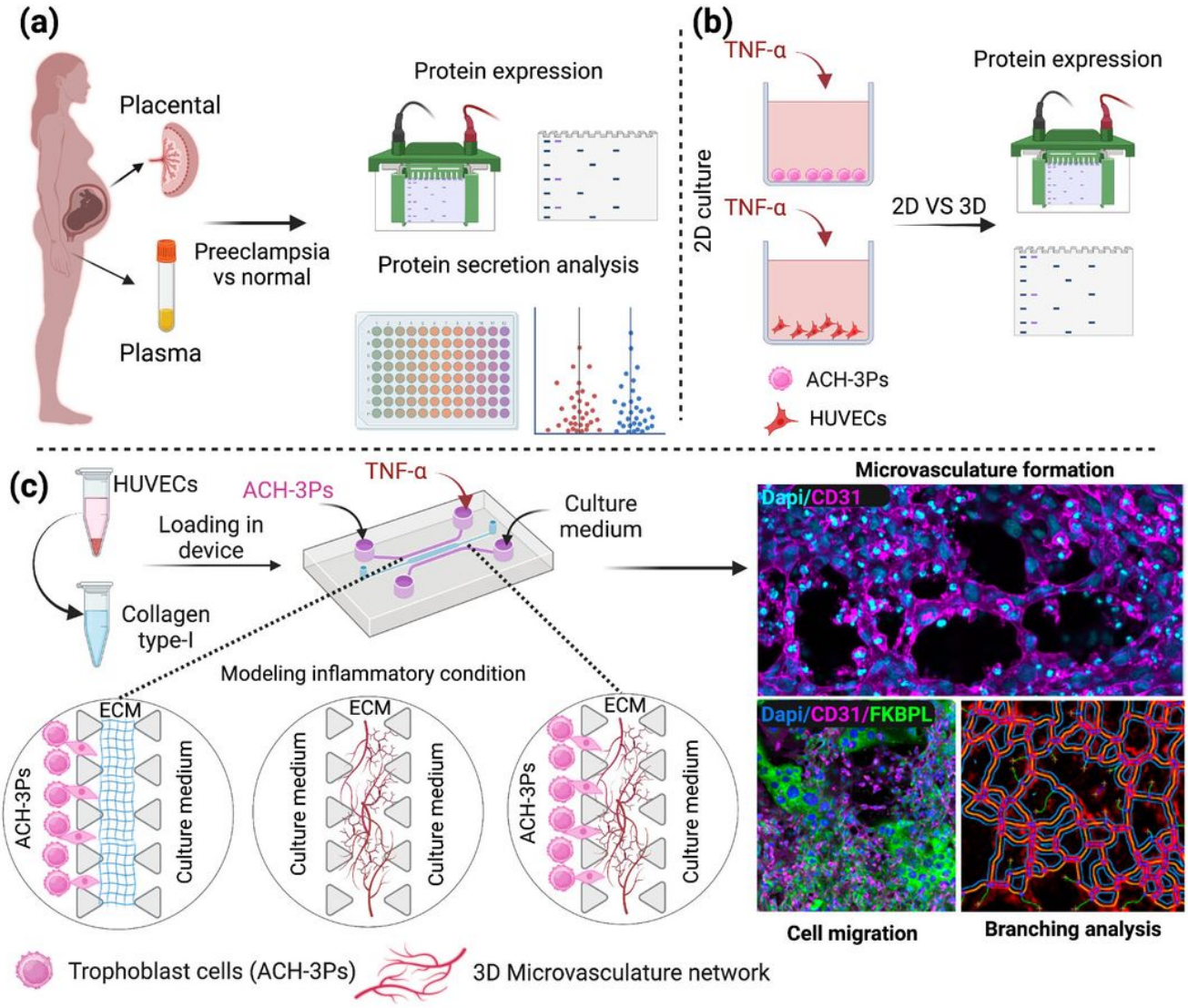

Figure 1

Schematic summary of the study design. (A) Human plasma and placental samples were interrogated for circulating and protein expression of FKBPL and Gal-3. (B) Two-dimensional monocultures of trophoblast (ACH-3Ps) and endothelial cells (HUVECs) were grown in the presence or absence of inflammatory stimuli, TNF-α, before protein expression was determined. (C) Placenta-on-a-chip was developed using 3D microfluidics chips to include HUVECs in the middle channel with ECM (Collagen type-I), and ACH-3Ps in the side channel that migrated across and integrated within vasculature.

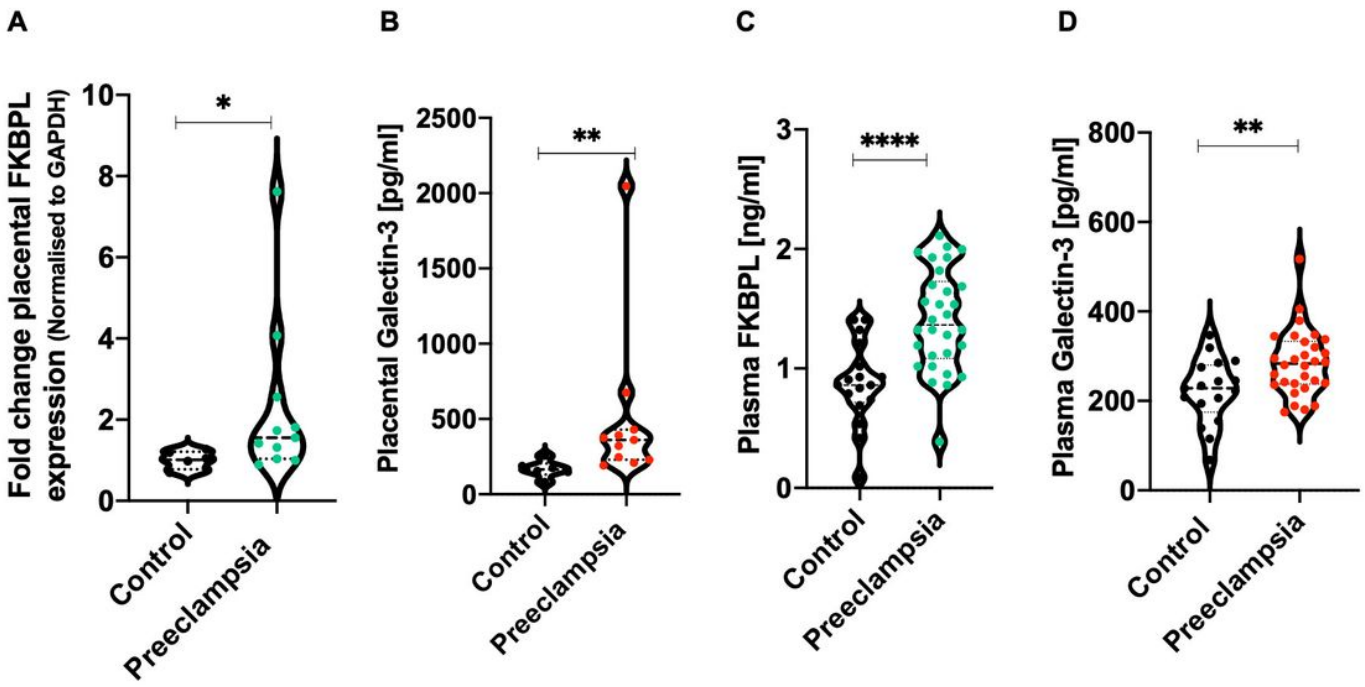

Figure 2

FKBPL and Gal-3 are increased in the placentae and plasma of women with preeclampsia. Protein lysates were generated from placental tissue collected from women with preeclampsia or normotensive controls. (A) FKBPL expression was determined by Western Blotting and normalized to GAPDH, the loading control. (B) Gal-3 levels from placental lysates were evaluated by enzyme-linked immunosorbent assay (ELISA). Data was plotted as mean ± SD; n≥6. (C & D) Plasma FKBPL and Gal-3 levels from women with preeclampsia vs normotensive controls were assessed by ELISA. Data plotted as mean ± SD; n≥17; unpaired student's t-test, *p<0.05, **p<0.01, ***p<0.001, ****p<0.0001.

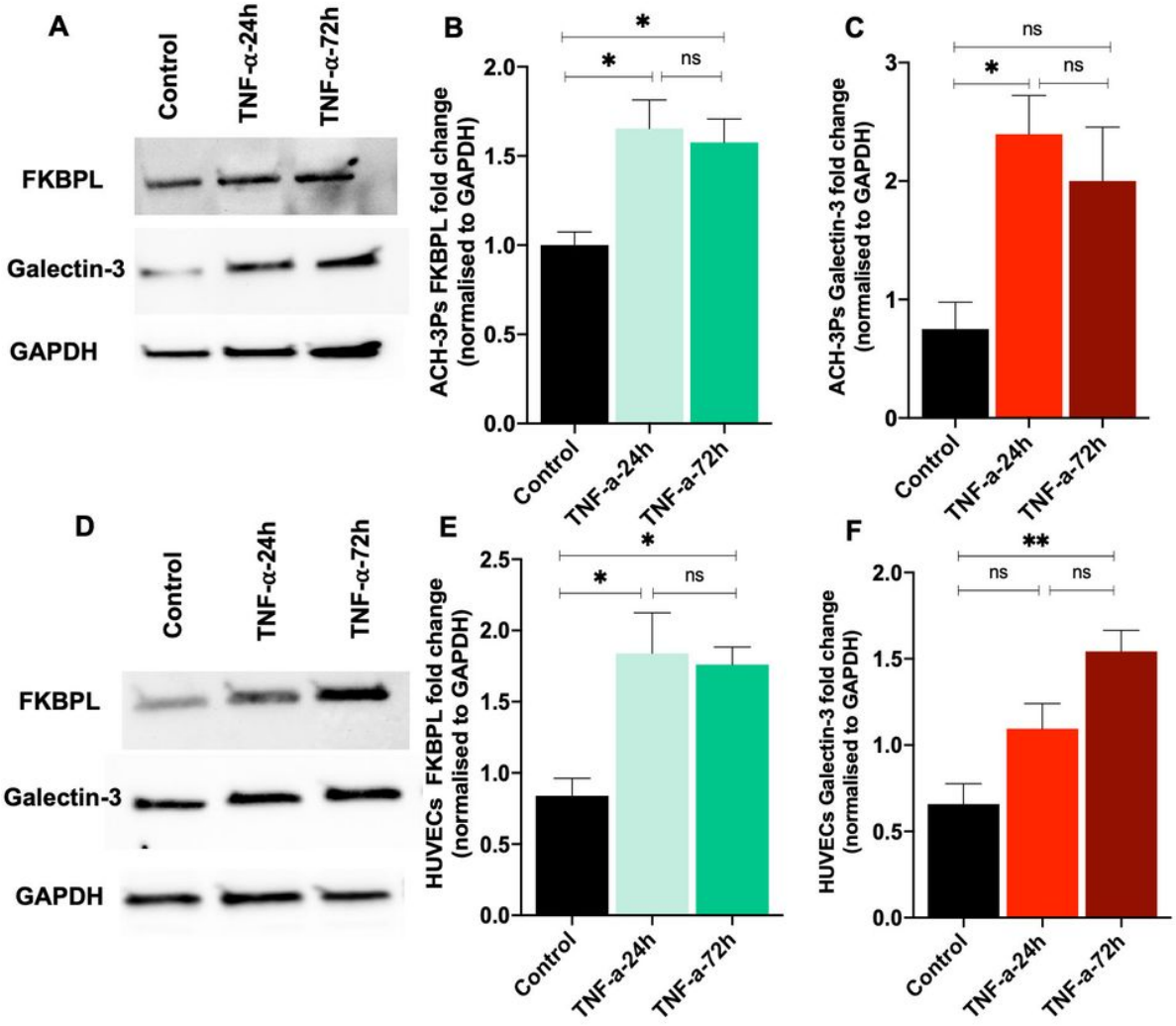

Figure 3

TNF-α treatment of trophoblasts and endothelial cells in 2D monocultures alters FKBPL and Galectin-3. (A-C) Western Blotting results of ACH-3Ps protein lysate expression of FKBPL and Gal-3. ACH-3Ps exposed to tumor necrosis factor alpha (TNF-α, 10ng/ml) for 24 or 72 hours. Control, untreated. GAPDH, loading control. (D-F) Western Blotting of HUVECs protein lysate showing expression of Gal-3 and FKBPL. HUVECs exposed to TNF-α (10ng/ml) for 24 or 72 hours. Control, untreated GAPDH, loading control. Data passed Shapiro-Wilk normality test and were analyzed by one-way analysis of variance (ANOVA) with Tukey post-hoc test; n=3; *p<0.05, ***p<0.001.

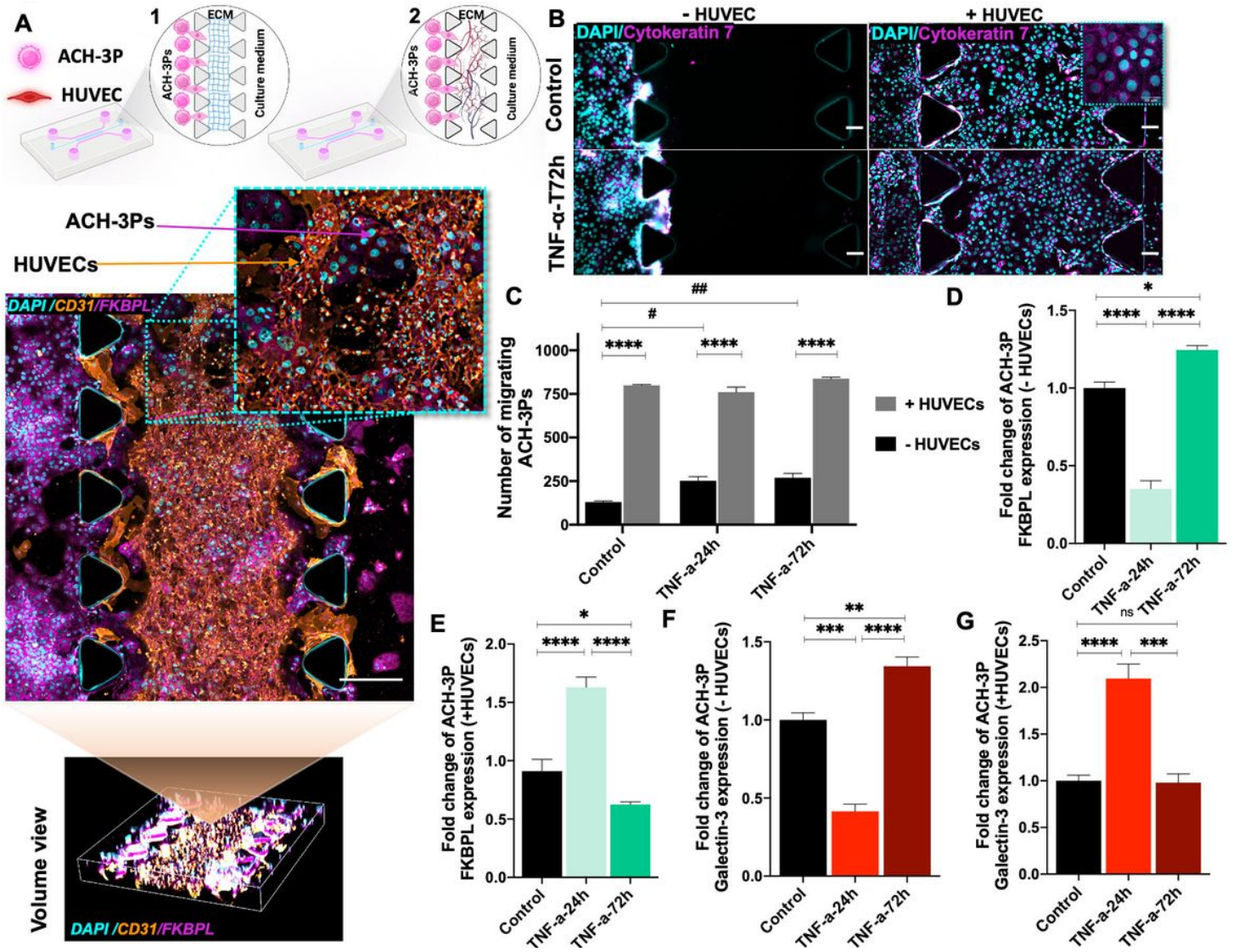

Figure 4

Endothelial cell presence and TNF-α modify trophoblast migration, as well as FKBPL and Gal-3 expression in a microfluidic chip. (A-1) Collagen matrix was added to the center channel and ACH-3Psto the left channel microfluidic chips. (A-2) In the co-culture set of chips, HUVECs were embedded within the center matrix channel and ACH-3Ps were added to the side channel. Representative immunofluorescence (IF) images of ACH-3Ps and HUVECs with high expression for FKBPL and CD31, respectively. (B) Representative IF images of ACH-3Ps invasion across the device (left to right) in the absence or presence of HUVECs and in normal or inflammatory conditions. Cells were IF stained for cytokeratin 7, a marker of trophoblasts, and DAPI. (C) Chips were treated with TNF-α (10ng/ml) for 24 or 72 hours, with untreated cells as a control. The number of migrating trophoblast cells from the left side channel were analyzed using ImageJ. (D) Chips were also fixed and stained by IF for quantification of FKBPL and Gal-3. The fold change of (D) FKBPL expression in ACH-3Ps without HUVECs and (E) with HUVECs. The fold change of (F) Gal-3 expression in ACH-3Ps without HUVECs and (G) with HUVECs Gal-3. Scalebars represent 100µm. Data plotted as mean fold change ± SEM, ordinary one-way ANOVA or two-way ANOVA with Tukey post-hoc test, n=3, *p<0.05, **p<0.01, ***p<0.001, ****p<0.0001.

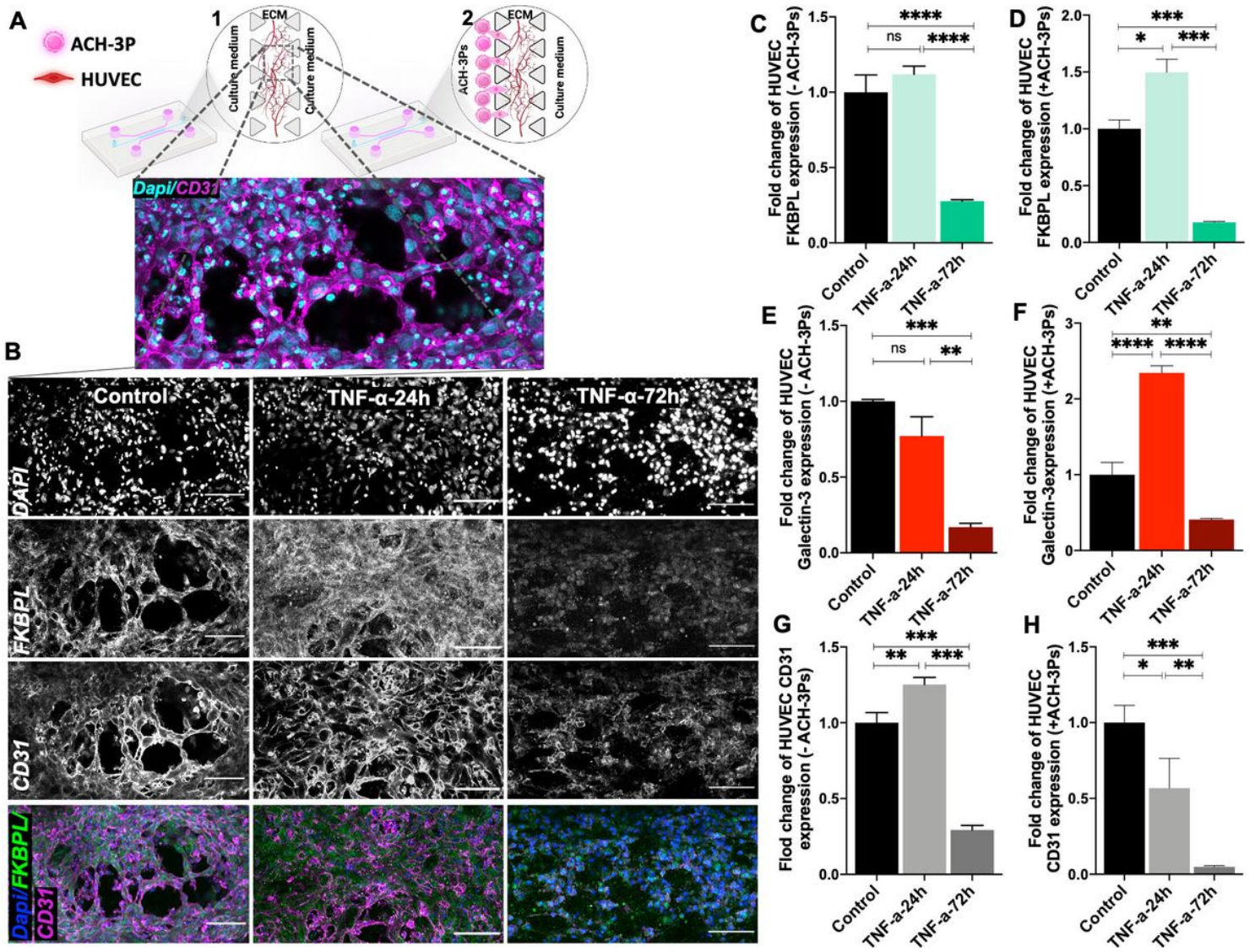

Figure 5

The presence of ACH-3Ps cells and inflammatory conditions impact vasculature formation and FKBPL, Gal-3 and CD31 expression in endothelial cells cultured in a microfluidic device. (A-1) HUVECs were combined with collagen matrix (2.5mg/ml) and added to the central channel of microfluidic chips. (A-2) In the co-culture set of chips, HUVECs were embedded within the center matrix channel and ACH-3Ps were added to the side channel. Chips were treated with TNF-α (10ng/ml) for 24 or 72 hours, with untreated cells as a control. Following 72 hours of culture, chips were probed for immunofluorescent imaging of FKBPL, CD31 and Gal-3. (A-B) Representative images of cells stained for DAPI, FKBPL and CD31. (C) FKBPL expression in HUVECs without ACH-3Ps and (D) with ACH-3Ps. The fold change of (E) Gal-3 expression in HUVECs without ACH-3Ps and (F) with ACH-3Ps. The fold change of (G) CD31 expression in HUVECs without ACH-3Ps and (F) with ACH-3Ps. Data presented as mean ± SEM, n=3, scalebar represents 100µm. Unpaired student's t-test and ordinary one-way ANOVA with Tukey post-hoc test for normally distributed data and Mann-Whitney or Kruskal-Wallis post-hoc test for non-normally distributed data; n=3; *p<0.05, **p<0.01, ***p<0.001, ****p<0.0001.

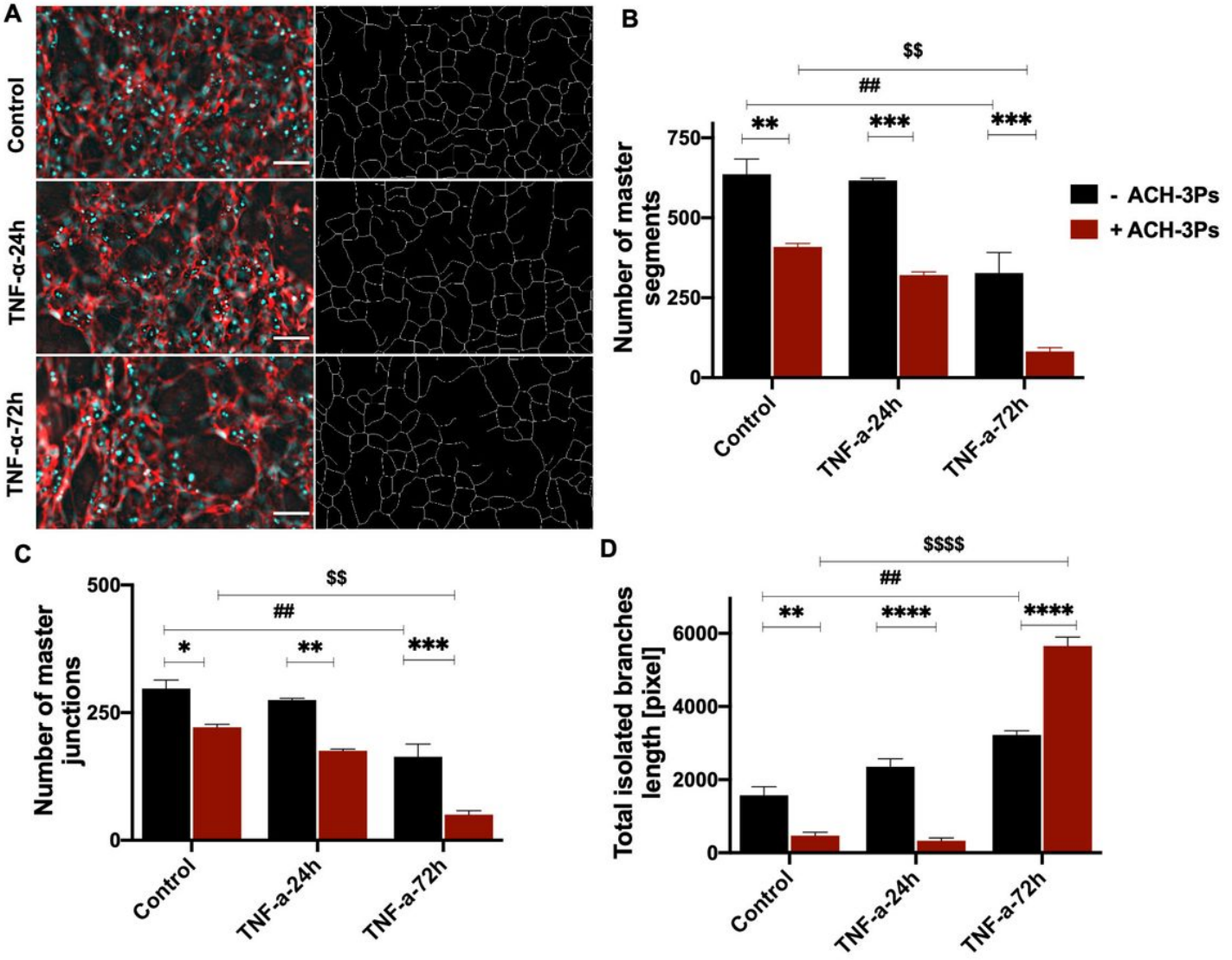

Figure 6

Quantification of microvascular network formation. (A) Representative immunofluorescent images of HUVECs in microfluidic devices under different TNF-α conditions, that were analyzed using the Angiogenesis Analyzer ImageJ macro and their corresponding map outputs. Scalebar represents 100μm. The (B) number of master segments (C) number of master junctions and (D) total isolated branches length of HUVECs with and without ACH-3Ps in the system. Data presented as mean ± SEM, n=3. Ordinary two-way ANOVA with Tukey post-hoc test; n=3; **p<0.01, ***p<0.001, ****p<0.0001.

Supplementary Files

This is a list of supplementary files associated with this preprint. Click to download.

- SupplementaryMaterial.pdf